6
tRNA Locations on the Ribosome

Knud H. Nierhaus

6.1
tRNAs Move through Functional Sites on the Ribosome

The ribosome harbors three well-defined binding sites for tRNAs: the A- and P-sites, where the aminoacyl- and peptidyl-tRNAs reside before peptide-bond formation, respectively, and the E-site, a site specific for deacylated tRNA from which the tRNA exits the ribosome. Localization of tRNA-related functional centers such as the PTF center or the decoding center on the ribosome has always been an important issue in the translational field. Many techniques have been used, developed and even invented to probe the interaction of tRNAs with the ribosome long before high-resolution structures became available.

Site-directed crosslinking (reviewed in Ref. [1]) of tRNAs identified the decoding site on the 30S and the PTF ring in the 50S subunit as functional centers. The anticodon loop of P-site bound tRNA crosslinks to C1400 (h44) of the 16S rRNA [2] and benzophenone attached to the amino acid of the P-site peptidyl-tRNA crosslinks to A2451 and C2452 and from the A-site peptidyl-tRNA to U2584 and U2585 with high yields [3]. In addition, various groups have shown that G2553 is located near the CCA end of an A-site substrate in the PTF center. This topological feature was convincingly confirmed by crosslinking the antibiotic puromycin, which functions as an analog of the tRNA acceptor end, to G2553. After crosslinking, the attached puromycin could still undergo peptide-bond formation [4]. A compilation of tRNA crosslinks can be found in the ribosomal crosslinking database (RDB [5]).

Distinct sets of rRNA bases have been assigned to contact tRNAs in A-, P- or E-sites by applying various techniques (Table 6-1). From the crystal structures of the 70S ribosome and the 30S subunit in the presence of tRNAs or tRNA fragments it is clear that most protections can be explained either by direct contacts with bases or by local conformational changes within the binding regions (discussed in depth in Ref. [6]). On the other hand, some of the P-site protections on the 30S subunit are actually E-site contacts. Protections of bases 1339, 1340 and 1381 are most probably caused by the backbone of the E-site tRNA and the protections in the 690 loop (h23) are caused by the anticodon loop of E-site bound tRNA (34–36). The 790 loop is a contact site for both E- and P-site tRNAs and the protection might result from either of these tRNAs. This mis-assignment has implications for the role of

Protein Synthesis and Ribosome Structure. Edited by K. H. Nierhaus and D. N. Wilson

ISBN 3-527-30638-2

Table 6-1 tRNA contacts with rRNA bases in the A-, P-, and E-sites

tRNA location / method	16S or 23S RNA / residues	Reference
A-site / protection	16S/530 loop: G529, G530, U531; helix 44: A1408, A1492, A1493, G1494; enhanced reactivity, helix 27: A892, G1405 23S/ A1439, C2254, A2439, A2451, G2553, pseudoU2555, A2602, U2609	37, 38, 7
A-site / site-directed muta-genesis	C74 of A-site tRNA base-pairs with G2553	39
P-site / protection	16S/ A532, G693, A794, C795, G926, G966, G1338, A1339, U1381 and in helix 44: C1399, C1400, G140123S/ A1916, A1918, U1926, G2251, G2253, A2439, A2451, G2505, U2506, U2584, U2585, A2602 (enhanced), and G2252 in the loop of H80, the P-loop	37, 38, 7
P-site / site-directed mutagenesis	C74 of P-site tRNA base-pairs with G2252 of H80 (P-loop)	40
P-site / interference	23S/modification of G2252, A2451, U2506, and U2585 prevents tRNA binding to the P-site	37
E-site / protection	23S/ G2112, G2116, A2169 at the L1-binding site; modification of C2394 interferes with E-site binding	7, 41, 42, 47

the E-site in ribosome function and consequences for the hybrid states model of elongation, a model that is interpreted on the basis of these protection experiments (see Chap. 8.1.1).

A ribosome discriminates tRNAs according to the coding sequence of the mRNA; however, during the translation process, they must be capable of binding between 33 and more than 50 (45 in *Escherichia coli*) different tRNA species; note that a tRNA species is defined solely by its anticodon. Thus the ribosome has to utilize conserved features of a tRNA to bind it. One such feature is the universally conserved CCA 3′-end of the tRNAs, which plays an important role in ribosome binding. Seventeen out of the 20 protections observed in the 23S rRNA with complete tRNAs are also seen with CCA fragments alone [7]. Furthermore, the binding of deacylated tRNAs to the E-site is dependent on an intact CCA end [8].

The first evidence that tRNAs do not interact exclusively using the anticodon loop and the CCA acceptor end, but instead are embedded in a ribosomal matrix, derives from phosphorothioate cleavage experiments. Iodine cleavage of phosphorothioated tRNAs bound to the ribosome yielded characteristic protection patterns [9, 10]. Since all tRNAs are conserved in terms of tertiary structure, at least some of the phosphate groups in the backbone might provide important binding determinants. In contrast with the protection pattern of the phosphorothioated mRNA, which locates only within the codon region [11], the cleavage patterns of

tRNAs bound to the ribosome are characteristic for their binding position and the functional state of the ribosome and cover the whole structure of a tRNA [9, 10]. In other words, the mRNA is hardly contacting the ribosome although about a sequence of 40 nt is covered by the ribosome [12, 13]. These rare contacts strikingly contrast with the extensive contacts of a tRNA, leading to the important conclusion that the tRNAs are actively transported during the translocation reaction, whereas the mRNAs are coupled with the movement of the tRNAs by the two adjacent codon–anticodon interactions (see Chap. 8.1).

The tRNA patterns, which differ significantly from the pattern of tRNAs in solution, have been interpreted to reflect the microtopography of the binding site, emphasizing intimate contacts between the ribosome and the entire tRNA surface. Contact patterns between tRNA nucleotides 29 and 43 (comprising anticodon loop and two adjacent stem base-pairs) are due to components of the 30S subunit, whereas the remaining 85% of the tRNA, viz. the acceptor stem, the T and D loops, is in contact with the 50S subunit. The 30S and 50S cleavage patterns are additive to yield the 70S pattern ([14, 15]; see Fig. 6-1A). Crystallographic data obtained with 30S subunits and 70S ribosomes [16, 6] are in perfect agreement with the 30S–50S contacts at the P-site of 70S ribosomes (Fig. 6-1B).

Phosphorothioated tRNAs bound to the ribosome yield two characteristic cleavage patterns: one observed in the P- or E-site (termed ε for its specific appearance at the E-site) and the other in the A- or the P-site (termed α for A-site; see also Chap. 8.1.2). The α- pattern shows few protection sites but several sites of enhancement, whereas, in contrast, the ε- pattern exhibits extensive protection sites and only few positions with enhanced iodine cleavage reactivity. This might reflect that the tRNAs bound at the E- and P-sites are buried in the ribosomal matrix to a higher extent than the A-site tRNA, an observation which is in agreement with the crystal structure of a programed 70S carrying tRNAs [6].

6.2
Visualization of tRNAs on the Ribosome

Biochemical studies have established that the ribosome has three tRNA-binding sites [17–20]. Contrary with this, three-dimensional (3D) cryo-EM has revealed five different tRNA positions on the ribosome, the classic A-, P-, and, E-sites and additional two sites termed P/E and E2 (see Table 6-4 and Refs. [21, 22] for a compilation of identified tRNA sites).

Two early cryo-EM studies identified three tRNA positions on the ribosome [23, 24]. The A-site was localized close to the L7/L12 stalk of the ribosome, the P-site tRNA spanning the inter-subunit space from the neck of the small subunit to the 50S subunit and the E-site tRNA was observed close to the mushroom-shaped L1 protuberance. Although the studies agreed on the position of the P-site tRNA, the locations of the A- and E-site tRNAs were remarkably different. The E-site puzzle was resolved by subsequent studies which showed that the E-site tRNA position was strongly dependent on buffer conditions, and the position of a single tRNA on the ribosome at the P-site on both the ionic conditions and the charging state of the tRNA [25, 26].

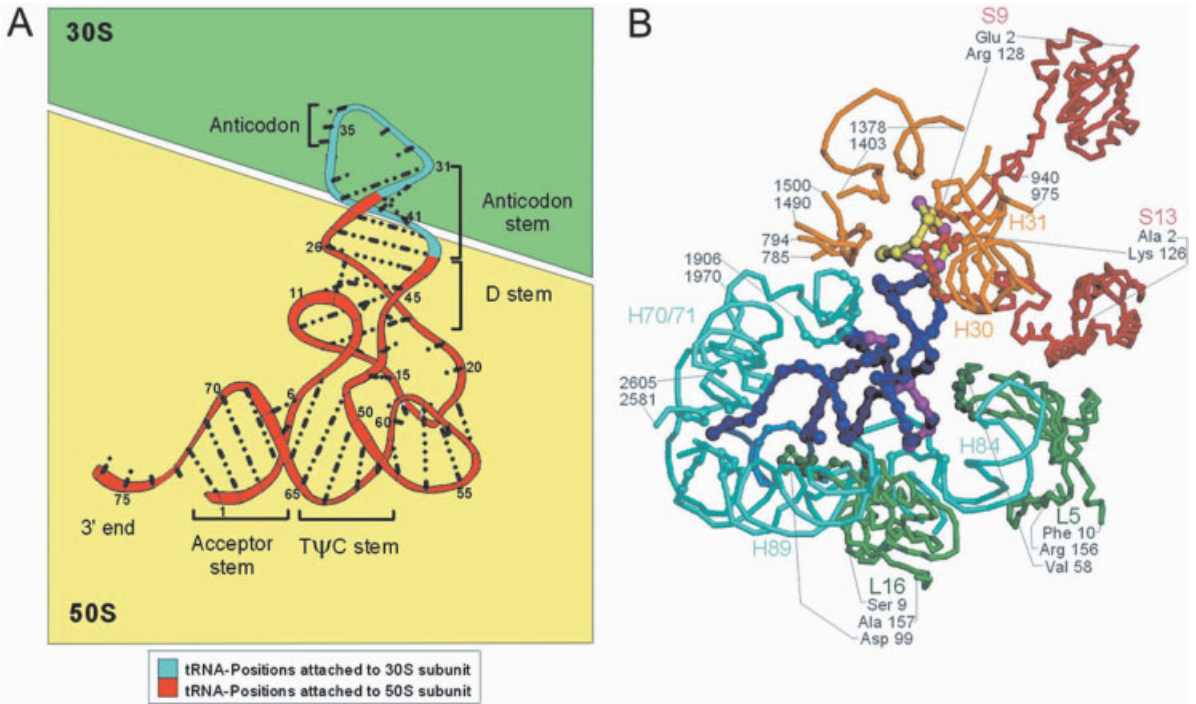

Figure 6-1 tRNA contacts with the ribosomal subunits at the P-site of 70S ribosomes. (A) Contact pattern obtained with protection experiments using phosphorothioated tRNAs (according to Ref. [15]). (B) Ribosomal components that come nearer than 10 Å to the tRNA at the P-site of the 70S ribosome (view from the E-site) according to Ref. [6]. The tRNA is colored: yellow, contacts with the small subunit; blue, contacts with the large subunit; pink, sites near to both tRNA and $tRNA^{Met}$ at the P-site according to Ref. [15]. Regions of the ribosomal components that are within a 10 Å proximity of the P-site tRNA are indicated with spheres. 30S components: gold, 16rRNA; red, S-proteins. 50S components: cyan, 23S rRNA; green, L-proteins.

A tRNA at the E-site was only observed under physiological buffer conditions, whereas under non-physiological conditions a tRNA was instead present at the E2 position that possibly represents an unstable intermediary state following release from the E-site and before dissociation from the 70S ribosome. A recent re-evaluation suggests that the E2 position might be even a misinterpretation caused by a conformational change of the L1 protuberance (C. M. T. Spahn, pers. comm.). Similarly, a tRNA at the hybrid site P/E was exclusively found under non-physiological conditions and thus probably represents a buffer artifact, but certainly not a ribosomal state with a significant population during the elongation cycle [25]; see Chap. 8.1.1 for discussion). We see that a critical discussion melts down the number of tRNA-binding sites on the ribosome again to the classical three sites, A, P, and E. The only exception of this view is the binding of the incoming ternary complex aa–tRNA•EF–Tu•GTP that has been termed A/T site (see, e.g., Fig 8-1; see also Ref. [27]). In fact, in this configuration, codon–anticodon interaction is checked at the decoding center of the A-site as a first step of the A-site occupation corresponding to the "low-affinity state" of the A-site in the allosteric three-site model (see Chap. 8.1.2).

An fMet-tRNA^{fMet} bound to the ribosomal P-site was visualized by cryo-EM at 15 Å and further refined to 11.5 Å [28, 29]. At 11.5 Å resolution, the tRNA X-ray structure could be fitted directly into an L-shaped P-site mass, oriented such that the CCA arm faces toward the entrance of the tunnel on the 50S subunit and the longer anticodon arm faces towards the cleft on small subunit [21]. The tRNA density makes four contacts with the ribosome. The backbone of G57, on the tip of the tRNA elbow, extends towards the 50S central protuberance, the C12–C23 base-pair on the D stem contacts both the 50S body and the 30S platform, and U33 and A37 in the anticodon loop extend into the 30S body and head [29]. The contact sites of the P-site tRNA seen in these cryo-EM studies [28] agreed well with the phosphate contact pattern derived from phosphorothioate studies mentioned in the preceding section [9].

On the 30S subunit, the anticodon ends of P- and A-site tRNAs before translocation (PRE state), as well as P- and E-sites after translocation (POST state), are in close proximity to one another (Figs. 6-2A and B), such that nucleotide 37 in the anticodon loops are 20 and 16 Å away from each other in the PRE and POST states, respectively. Following peptide-bond formation the CCA ends of P- and A-site tRNAs are 17 Å apart (see Chap. 8.4 for more details), whereas after translocation the CCA end of E-site tRNA is turned towards the L1 stalk and measures 60 Å from the P-site CCA end. The position of the CCA end at the E-site has been determined in crystals of 50S subunits of the archeon *Haloarcula marismortui* [30]. The fixation differs from those observed in A- and P-sites, where the CCA ends are held via Watson–Crick base pairs with the rRNA. Instead, at the E-site, the A76 is fixed by an intricate network of hydrogen bonds to nucleotides conserved in all three kingdoms of life (Fig. 6-3): A76 is hydrogen-bonded to C2394 (*E. coli* nomenclature) and to the phosphooxygen of A2422, the sugar-phosphate backbone of 76 to C2394. Furthermore, A76 is stacked between G2421 and A2422 (Fig. 6-3). The tight packing of A76 at the E-site leaves no room for an amino acid linked to the A76 via an ester bond and thus explains the earlier finding that this site is specific for deacylated tRNA [20], and that

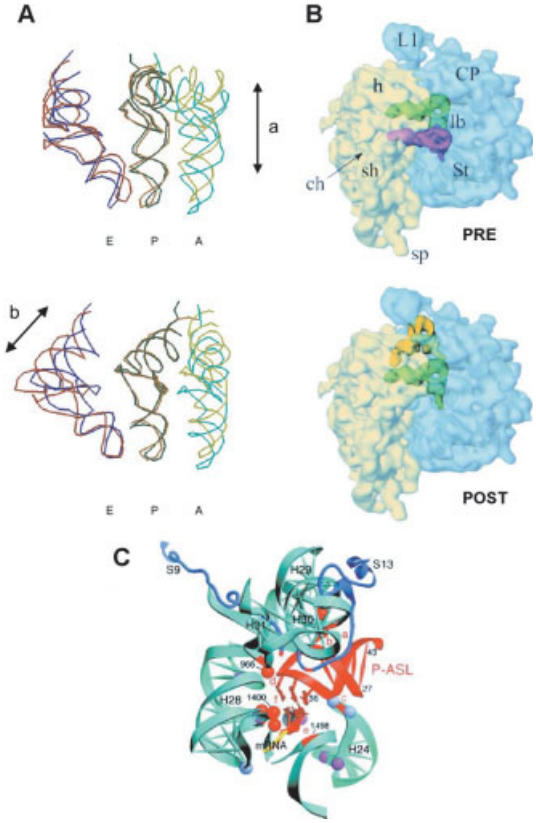

Figure 6-2 tRNA positions on the ribosome. (A) Relative positions of the three tRNAs bound at the A-, P- and E-sites. The P and C1′ atoms of the P-site tRNAs are used to align the molecules of the cryo-EM (brown) with that from the X-ray work (dark green; Refs. [21, 6]). The two studies agree on the position of the tRNAs on the ribosome. From this comparison it can be seen that the A-site tRNAs (cryo-EM in olive green, X-ray in cyan) are shifted relative to each other along the anticodon stem axis (arrow a), and the E-site-bound tRNAs along the acceptor stem axis (arrow b, cryo-EM in red and X-ray in blue). Note that the anticodon regions of all three tRNAs are in close proximity to each other. (B) tRNAs in the PRE and the POST states of the *E. coli* ribosome. Cryo-EM reconstructions of tRNAs bound to the 70S ribosome. PRE state: tRNAs bound to the A-site (pink) and P-site (green). POST state: tRNAs bound to the P-site (green) and E-site (yellow). The small 30S subunit is shown in yellow, the large 50S subunit in blue. To demonstrate the tRNA positions, the 70S ribosome is presented as a semitransparent surface. (C) Fixation of the codon–anticodon duplex at the ribosomal P-site according to Ref. [6]. The 16S rRNA is shown in cyan, ribosomal protein S13 in blue and the anti-codon stem-loop of the P-site tRNA in red. 16S rRNA contacts with the P-site tRNA are indicated and labeled in red (a–f).

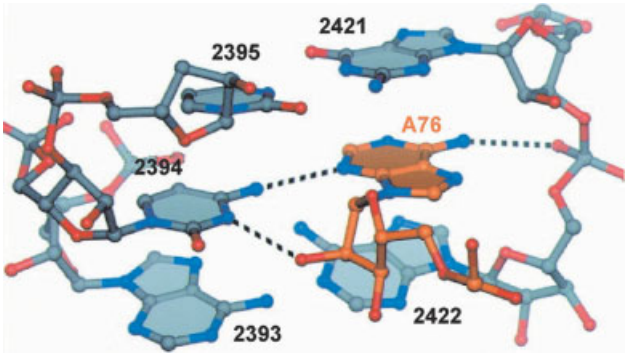

Figure 6-3 A76 of the CCA end at the E-site is held by network of hydrogen bonds. For details see text (taken from Ref. [30]).

a tRNA at the E-site requires an intact CCA end [8]. Only CCA-Gly, the smallest aminoacyl residue, could possibly fit into the E-site. However, this possibility is not relevant for protein synthesis, since there is always a deacylated tRNA at the P-site before translocation and after peptide-bond formation (see, e.g., models of the elongation cycle; Figs. 8.2A and B). The only situation where an aminoacyl-tRNA binds directly to the ribosome is during initiation and here, as mentioned, the fMet moiety itself would prevent the tRNA from binding at the E-site and probably the involvement of the initiation factors for directing this binding would provide further protection against this.

The final two nucleotides of the CCA end of an E-tRNA pass through a loop of protein L44e. Although L44e does not exist in bacteria, the bacterial protein L33 mimics the shape of the globular part of L44e and L31, the extended part of L44e. In fact, it may be the case that binding of a CCA at the E-site of bacterial ribosomes would entail the insertion through the loop extension of L31, although whether this similarity in the involvement of the loop region of the ribosomal proteins is functionally significant is unclear. Since the fold of L31 and L33 is significantly different from that of L44e, whereas the critical C2395 is conserved in over 99% of all species, the authors suspect that the last universal common ancestor (LUCA) fixed the CCA end of the E-tRNA via rRNA, and that protein components were added after separation into kingdoms [30].

Notably, a P-site tRNA occupies virtually the same position in the ribosome before and after translocation (PRE and the POST states, respectively). The angles between the tRNAs in the PRE at A- and P-sites and in the POST state at P- and E-sites are 39° and 35°, respectively [21].

Combined crystal structures of three different tRNA 70S complexes at 7.8 and 5.5 Å resolution yields a wealth of information regarding tRNA–ribosome interactions for all three sites [31, 6] (see Table 6-2 [15]). The positions of the tRNAs on the ribosome are in good agreement with those from the cryo-EM work of Frank and colleagues [21] concerning authentic PRE and POST states of ribosomes,

Table 6-2 Contact sites with tRNA phosphates at the P-site that were strongly protected against iodine (I_2) access in two different elongator tRNAs, viz. $tRNA^{Phe}$ and elongator $tRNA^{Met}$ (adapted from Ref. [15])

5′-phosphate of tRNA base	Residue of rRNA or r-protein nearer than 10 Å (rRNA/nt or r-prot/aa; see Ref. [6])	Evolutionary conservation (in percent of species)	
		Eubact.	Three domains
Y11	23S/1909, 1910, 1923, 1924	80–90, ≥95, ≥95, ≥95	<80, 90–95, ≥95, <80
G30	16S/1230	≥95	80-90
	S13/Lys121	Lys or Arg at position 120	
Y32	16S/1341	≥95	≥95
	S9/Ser126, Lys127, Arg128	126 and 127: ~50% cons. 128: ~90% conserved	
G34	(anticodon)		
C41	16S/1339, 1340	≥95, <80	≥95, <80
T54	23S/2280, 2327	≥95, ≥95	80-90, <80
C56	L5/Arg56 and Glu65	Arg or Lys at positions 56 and 64	
A58	Protected via tertiary folding of tRNA		
U59	Protected via tertiary folding of tRNA		
Y60	Protected via tertiary folding of tRNA		

Note: nt, nucleotidyl residue; aa, aminoacyl residue, eubact., eubacterial domain; three domains, the eubacterial, archeal and eukaryotic domains. The conservation data concerning rRNA were obtained from The Gutell Lab Pages (www.rna.icmb.utexas.edu/csi), the sequences of the ribosomal proteins (r-prot.) were obtained from the Sequence Retrieval System (www.expasy.ch/srs5/), the alignment followed Ref. [43] according to www.expasy.ch/srs5/.

although closer inspection of the relative orientations reveal some minor deviations. In Fig. 6-2(A), the P-site tRNA molecules of the cryo-EM [21] and the X-ray studies [6] are aligned for comparison. In the crystallographic study, the P-site-bound $tRNA^{fMet}$ is slightly kinked at the D stem–anticodon junction in comparison with the X-ray structure of the free tRNA that was used to fit the cryo-EM map. In both the cryo-EM with 12–17 Å resolution and the X-ray analysis with 5–7 Å resolution single-stranded RNA cannot be unequivocally identified, and thus the 3′ single-stranded end of $tRNA^{fMet}$ was deduced from the highly resolved tRNA crystal structure (see, e.g., Ref. [32]). Alignment of the crystal and cryo-EM maps based on the P-site tRNA positions shows the A- and E-site tRNAs in slightly different positions. The A-site tRNAs are shifted with respect to each other along the anticodon stem axes and the E-site tRNAs along the acceptor stem axes. The E-site tRNA in the X-ray study was reported to be substantially distorted [6] relative to the X-ray structure of the free tRNA that was used to fit the cryo-EM data. The distortion might be

due to the fact that the E-site-bound tRNA is non-cognate and thus cannot undergo base-pairing with the E-site codon of the mRNA. Note that during an elongation cycle a deacylated tRNA at the E-site is always a cognate one. The juxtaposition of codon and anticodon at the E-site of the 70S crystal structure makes it probable that under physiological conditions codon–anticodon interaction occurs at this site in agreement with biochemical data [33–35].

6.3 tRNA–ribosome Contacts

In this section, we will consider in detail the contacts of a tRNA at each of the three tRNA-binding sites A, P and E.

Ramakrishnan and colleagues [16] presented the first high-resolution view at 3.1 Å of the P- and A-site tRNA interactions with the 30S subunit. Fortuitously, crystal packing of the *T. thermophilus* 30S subunits placed the spur (h6) of one subunit in the P-site of another, thereby mimicking the anticodon stem-loop of a P-site-bound tRNA. Remarkably, the mRNA base-pairing partner was provided by the 3′-end of 16S rRNA which, folding back upon itself, extended into the decoding center. These crystals were then soaked with an anticodon stem-loop fragment of a tRNA (ASL-tRNA) and a six base poly(U) mRNA fragment to include A-site interactions within the scope of these studies [36]. At the A-site, the ribosome scans the mRNA–tRNA codon–anticodon base-pairing to ensure high-fidelity decoding of aa-tRNAs and to maintain the reading frame (refer Chap. 8.2; [36]).

On the small subunit, the P-site-bound tRNA is fixed very tightly via six interactions with the 16S RNA. RNA elements 1338–1341 (hydrogen bonding to bases) and 1229–1230 (sugar-phosphate backbone) of the 16S rRNA interact in the minor groove of the acceptor stem. Only one hydrogen bond appears to be base-specific. The interaction is supported by the C-terminal tails of proteins S13 and S9. The base corresponding to tRNA position 34 is stacked on C1400, whereas A790 packs against tRNA positions 40 and 41. The P-site codon–anticodon helix is positioned in the major groove of the penultimate helix (h44) and is fixed with a number of "ribosomal fingers" mainly to the sugar-phosphate backbone (Fig. 6-2C; see Table 6-2 for P-site contacts of the ribosome with two different elongator tRNAs; for involvement of h44, bases A1492 and A1493, in the decoding mechanism see Chap. 8.2).

Comprehensive analyses of tRNA:ribosome interactions have been described by Noller and colleagues on the basis of *T. Thermophilus* 70S tRNA co-crystals [31, 6]. A- and P-site tRNAs exhibit similar modes of interaction with the large ribosomal subunit. The 23S rRNA helices, H80-81 in the P-site and H89 in the A-site run parallel to the acceptor stem of the tRNAs making minor groove–minor groove contacts. Proteins, L5 and L16 in A- and P-sites respectively, contact the T-loop at the elbow of the tRNA. Additionally, the A-site finger (H38) contacts the elbow (D and T loops) of the A-site tRNA. H69 and H93 fix both tRNAs simultaneously: helix 69 is "sandwiched" between the top of the D-stem of the P-site tRNA (from the minor groove side) and the D-stem of the A-site tRNA from the major groove side, whereas H93 squeezes between the respective CCA ends. In accordance with bio-

chemical data, G2553 in H89 is positioned to base-pair with C75 of the A-site tRNA, whereas G2252 in H80 base-pairs with C74 of P-site-bound tRNA.

The E-site on the 30S subunit contains proteins S7 and S11, a highly conserved β–hairpin of S11 contacts the backbone of the anticodon stem, whereas α-helix 6 of S7 faces the anticodon side of the anticodon loop. 16S rRNA contacts include h29 (1339, 1340), h28 (1382), the 690 loop, and 790 loop [6].

In the large subunit, the E-site tRNA forms protein contacts at the elbow in similar fashion to the A- and P-site tRNAs. The elbow neighbors protein L1 and H77 of 23S RNA, i.e., both elements that constitute the characteristic L1 protuberance. Other E-site tRNA:23S rRNA contacts are seen with nucleotides 1–5 and 71–76 at the end of the acceptor stem that is buried in a deep pocket made of RNA and protein L33. Here minor groove–minor groove interactions with H68 are evident as well as several interactions with H11, H74, H75, and protein L33.

References

1 R. Brimacombe, *Eur. J. Biochem.* **1995,** *230,* 365–383.
2 J. B. Prince, B. H. Taylor, D. L. Thurlow et al., *Proc. Natl. Acad. Sci. USA* **1982,** *79,* 5450–5454.
3 A. Barta, E. Kuechler, G. Steiner: in *The Ribosome: Structure, Function and Evolution,* eds W. E. Hill, A. Dahlberg, R. A. Garrett et al., American Society for Microbiology, Washington, DC 1990, 359–365.
4 R. Green, C. Switzer, H. Noller, *Science* **1998,** *280,* 286–289.
5 P. V. Baranov, P. V. Sergiev, O. A. Dontsova et al., *Nucleic Acids Res.* **1998,** *26,* 187–189.
6 M. M. Yusupov, G. Z. Yusupova, A. Baucom et al., *Science* **2001,** *292,* 883–896.
7 D. Moazed, H. F. Noller, *Proc. Natl. Acad. Sci. USA* **1991,** *88,* 3725–3728.
8 R. Lill, A. Lepier, F. Schwägele et al., *J. Mol. Biol.* **1988,** *203,* 699–705.
9 M. Dabrowski, C. M. T. Spahn, K. H. Nierhaus, *EMBO J.* **1995,** *14,* 4872–4882.
10 M. Dabrowski, C. M. T. Spahn, M. A. Schäfer et al., *J. Biol. Chem.* **1998,** *273,* 32793–32800.
11 E. V. Alexeeva, O. V. Shpanchenko, O. A. Dontsova et al., *Nucleic Acids Res.* **1996,** *24,* 2228–2235.
12 D. Beyer, E. Skripkin, J. Wadzack et al., *J. Biol. Chem.* **1994,** *269,* 30713–30717.
13 G. Z. Yusupova, M. M. Yusupov, J. H. Cate et al., *Cell* **2001,** *106,* 233–241.
14 K. H. Nierhaus, C. M. T. Spahn, N. Burkhardt et al.: in *The Ribosome. Structure, Function, Antibiotics, and Cellular Interactions,* eds R. A. Garrett, S. R. Douthwaite, A. Liljas et al., ASM Press, Washington, DC 2000, 319–335.
15 M. A. Schäfer, A. O. Tastan, S. Patzke et al., *J. Biol. Chem.* **2002,** *277,* 19095–19105.
16 A. P. Carter, W. M. Clemons, D. E. Brodersen et al., *Nature* **2000,** *407,* 340–348.
17 R. A. Grajevskaja, Y. V. Ivanov, E. M. Saminsky, *Eur. J. Biochem.* **1982,** *128,* 47–52.
18 R. Lill, J. M. Robertson, W. Wintermeyer, *Biochemistry* **1984,** *23,* 6710–6717.
19 K. H. Nierhaus, *Mol. Microbiol.* **1993,** *9,* 661–669.
20 H.-J. Rheinberger, H. Sternbach, K. H. Nierhaus, *Proc. Natl. Acad. Sci. USA* **1981,** *78,* 5310–5314.
21 R. K. Agrawal, C. M. T. Spahn, P. Penczek et al., *J. Cell. Biol.* **2000,** *150,* 447–459.

22 C. M. T. Spahn, K. H. Nierhaus, *Biol. Chem.* **1998**, *379*, 753–772.
23 R. K. Agrawal, P. Penczek, R. A. Grassucci et al., *Science* **1996**, *271*, 1000–1002.
24 H. Stark, E. V. Orlova, J. Rinke-Appel et al., *Cell* **1997**, *88*, 19–28.
25 R. K. Agrawal, A. B. Heagle, P. Penczek et al., *Nat. Struct. Biol.* **1999**, *6*, 643–647.
26 G. Blaha, U. Stelzl, C. M. T. Spahn et al., *Meth. Enzymol.* **2000**, *317*, 292–309.
27 M. Valle, J. Sengupta, N. K. Swami et al., *EMBO J.* **2002**, *21*, 3557–3567.
28 I. S. Gabashvili, R. K. Agrawal, C. M. T. Spahn et al., *Cell* **2000**, *100*, 537–549.
29 A. Malhotra, P. Penczek, R. K. Agrawal et al., *J. Mol. Biol.* **1998**, *280*, 103–116.
30 T. M. Schmeing, P. B. Moore, T. A. Steitz, *RNA* **2003**, *9*, 1345–1352.
31 J. H. Cate, M. M. Yusupov, G. Z. Yusupova et al., *Science* **1999**, *285*, 2095–2104.
32 S. H. Kim, F. L. Suddath, G. J. Quigley et al., *Science* **1974**, *185*, 435–440.
33 H.-J. Rheinberger, K. H. Nierhaus, *FEBS Lett.* **1986**, *204*, 97–99.
34 H.-J. Rheinberger, H. Sternbach, K. H. Nierhaus, *J. Biol. Chem.* **1986**, *261*, 9140–9143.
35 F. J. Triana–Alonso, K. Chakraburtty, K. H. Nierhaus, *J. Biol. Chem.* **1995**, *270*, 20473–20478.
36 J. M. Ogle, D. E. Brodersen, W. M. Clemons Jr et al., *Science* **2001**, *292*, 897–902.
37 M. Bocchetta, L. Xiong, A. S. Mankin, *Proc. Natl. Acad. Sci. USA* **1998**, *95*, 3525–2530.
38 D. Moazed, H. F. Noller, *Nature* **1989**, *342*, 142–148.
39 D. Kim, R. Green, *Mol. Cell.* **1999**, *4*, 859–864.
40 R. R. Samaha, R. Green, H. F. Noller, *Nature* **1995**, *377*, 309–314.
41 M. Bocchetta, S. Gribaldo, A. Sanangelantoni et al., *J. Mol. Evol.* **2000**, *50*, 366–380.
42 D. Moazed, H. F. Noller, *Cell* **1989**, *57*, 585–597.
43 F. Corpet, *Nucl. Acids Res.* **1988**, *16*, 10881–10890.